Nuclear Engineering and Technology 48 (2016) 1412–1422

Available online at ScienceDirect

Nuclear Engineering and Technology

journal homepage: www.elsevier.com/locate/net

Original Article

# Round Robin Analyses on Stress Intensity Factors of Inner Surface Cracks in Welded Stainless Steel Pipes

*Chang-Gi Han* [a], *Yoon-Suk Chang* [a,*], *Jong-Sung Kim* [b], *and Maan-Won Kim* [c]

[a] *Department of Nuclear Engineering, College of Engineering, Kyung Hee University, 1732 Deogyeong-daero, Giheung-gu, Yongin-si, Gyeonggi-do 446-701, Republic of Korea*

[b] *Department of Mechanical Engineering, Sunchon National University, 255 Jungang-ro, Suncheon-si, Jeollanam-do 540-950, Republic of Korea*

[c] *Central Research Institute, Korea Hydro & Nuclear Power Company, 70 Yuseong-daero, 1312 Beon-gil, Yuseong-gu, Daejeon 305-343, Republic of Korea*

ARTICLE INFO

*Article history:*
Received 4 December 2015
Received in revised form
21 April 2016
Accepted 24 May 2016
Available online 16 June 2016

*Keywords:*
Finite Element Analyses
Fitness-for-Service Assessment Codes
Inner Surface Crack
Stress Intensity Factor
Welding Residual Stress

ABSTRACT

Austenitic stainless steels (ASSs) are widely used for nuclear pipes as they exhibit a good combination of mechanical properties and corrosion resistance. However, high tensile residual stresses may occur in ASS welds because postweld heat treatment is not generally conducted in order to avoid sensitization, which causes a stress corrosion crack. In this study, round robin analyses on stress intensity factors (SIFs) were carried out to examine the appropriateness of structural integrity assessment methods for ASS pipe welds with two types of circumferential cracks. Typical stress profiles were generated from finite element analyses by considering residual stresses and normal operating conditions. Then, SIFs of cracked ASS pipes were determined by analytical equations represented in fitness-for-service assessment codes as well as reference finite element analyses. The discrepancies of estimated SIFs among round robin participants were confirmed due to different assessment procedures and relevant considerations, as well as the mistakes of participants. The effects of uncertainty factors on SIFs were deducted from sensitivity analyses and, based on the similarity and conservatism compared with detailed finite element analysis results, the R6 code, taking into account the applied internal pressure and combination of stress components, was recommended as the optimum procedure for SIF estimation.

Copyright © 2016, Published by Elsevier Korea LLC on behalf of Korean Nuclear Society. This is an open access article under the CC BY-NC-ND license (http://creativecommons.org/licenses/by-nc-nd/4.0/).

* *Corresponding author.*
E-mail address: yschang@khu.ac.kr (Y.-S. Chang).

http://dx.doi.org/10.1016/j.net.2016.05.006

1738-5733/Copyright © 2016, Published by Elsevier Korea LLC on behalf of Korean Nuclear Society. This is an open access article under the CC BY-NC-ND license (http://creativecommons.org/licenses/by-nc-nd/4.0/).

## 1. Introduction

As operating years of nuclear power plants have increased, various aging degradations have been reported in major components and piping systems so that establishment of appropriate evaluation methods are required. Austenitic stainless steels (ASSs) are widely used in nuclear pipes of nuclear power plants as they exhibit a good combination of mechanical properties and corrosion resistance. Since post-weld heat treatment of ASS welds has not been carried out to avoid sensitization [1], high tensile residual stresses may occur in the ASS welds and the resulting high tensile residual stress field contributes to one of the crack driving forces [2]. Furthermore, recent research has reported that ASS welds lose toughness due to thermal aging embrittlement [3,4]. However, since there has been significant deviation among well-known fitness-for-service (FFS) codes and equations, as well as analysts, due to the inherent complexity of the welding, the effects of residual stresses on cracking behavior in ASS welds should be evaluated rigorously prior to dealing with the embrittlement phenomenon.

Fracture mechanics parameters, such as stress intensity factors (SIFs), are commonly used to evaluate the integrity of cracked pipes and other components in the nuclear industry. While a lot of research works on SIFs and welding residual stresses of Ni-based alloy steels have been carried out [5–8], there were few investigations into welded ASS pipes. This is because they have sufficiently high ductility and resistance to brittle fracture. FFS assessment codes such as American Society of Mechanical Engineers (ASME)

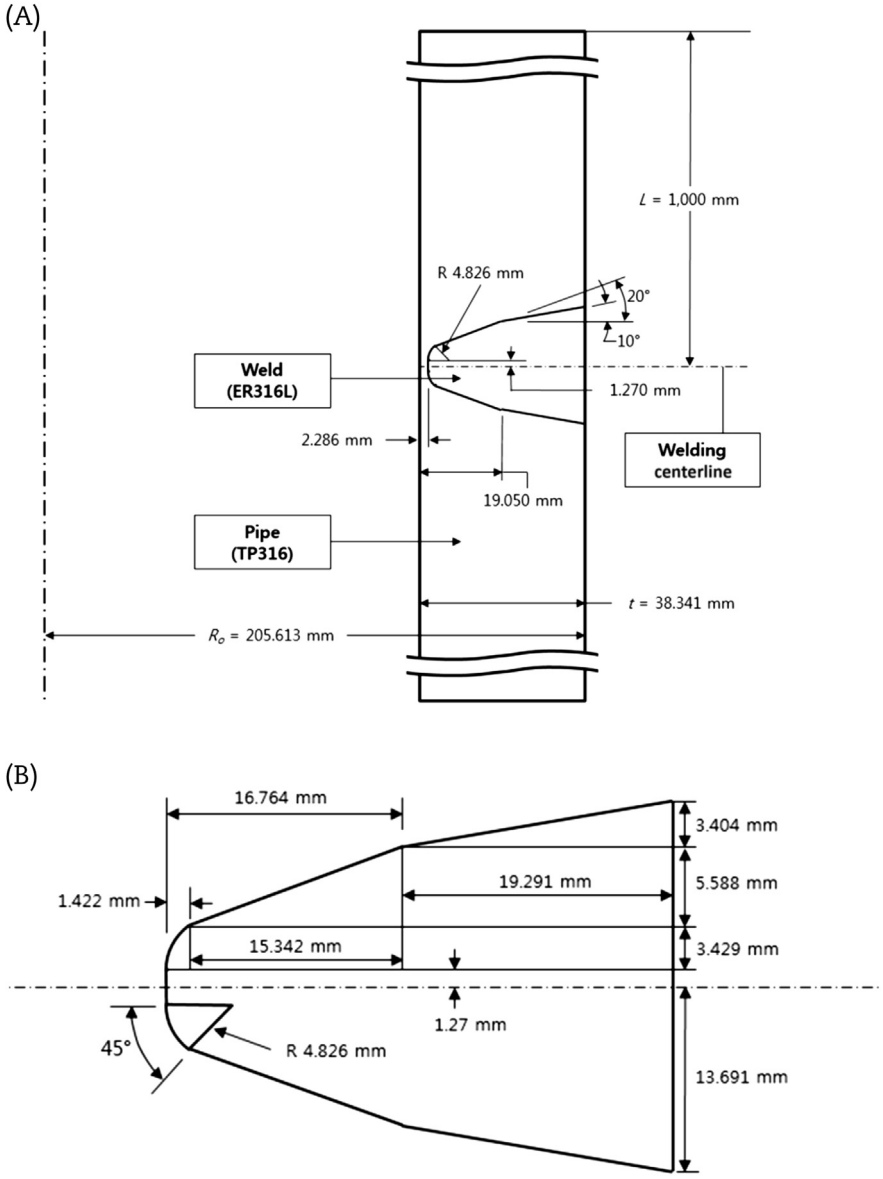


**Fig. 1 – Schematics of an ASS pipe and its weldment [14]. (A) Geometry of an ASS pipe. (B) Enlarged geometry of a weldment. ASS, austenitic stainless steel.**

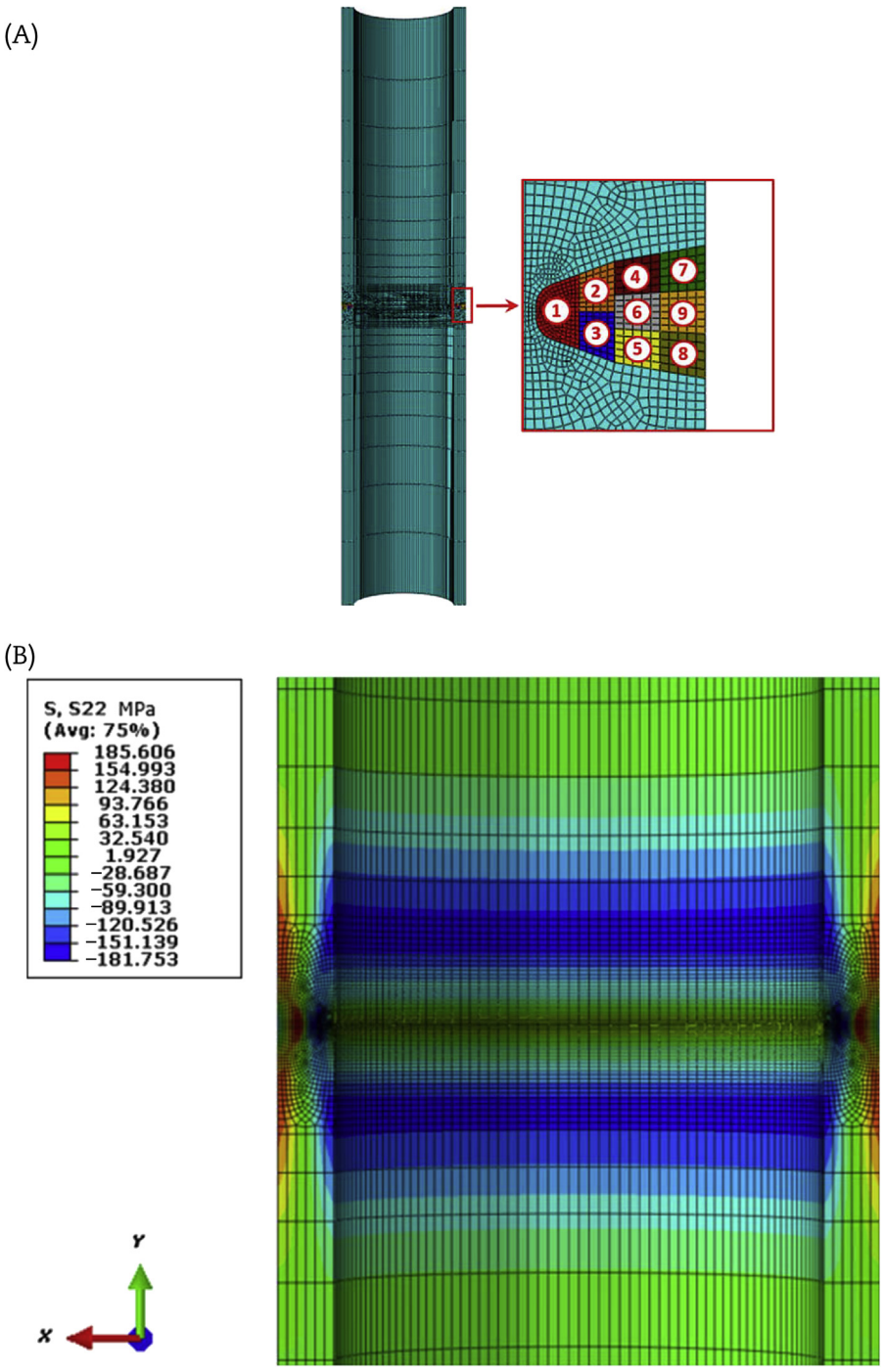


**Fig. 2 – Three-dimensional FE model and a representative residual stress analysis result. (A) Three-dimensional FE model and welding beads. (B) Axial stress distribution after the welding. FE, finite element.**

Boiler and Pressure Vessel Code, Section XI (hereafter, ASME Sec. XI) [9], American Petroleum Institute (API) 579-1 [10], and R6 [11] suggest SIF evaluation procedures for crack integrity assessment. A benchmark for the analytical calculation of fracture mechanics parameters for cracked pipes and components, proposed in the framework of the Organization for Economic Cooperation and Development/ Working Group on Integrity and Ageing of Components and Structures, has been carried out to compare different estimation schemes according to various FFS assessment codes, with reference analyses conducted by the finite element (FE) method [12,13]. The benchmark results showed very good homogeneity for both the AFCEN (Association Française pour les règles de conception, de construction et de

surveillance ex exploitation des matériels des Chaudières Electro-Nucléaires) code and the R6 code, and large discrepancies for the ASME code.

In the present study, round robin (RR) SIF analyses for ASS pipes with semicircular and fully circumferential inner surface cracks were conducted by three organizations. Typical stress profiles were generated by considering residual stresses and normal operating conditions of a representative pressurized water reactor. Each participant estimated SIFs through three-dimensional (3-D) FE analyses or FFS assessment codes, and resulting values were compared. Moreover, sensitivity analyses were carried out by the organizer to examine the effects of analysis techniques and variables such as fitting of stress distribution, considerations of internal pressure, and combination of SIFs.

## 2. Problems and reference solutions

### 2.1. *Description of RR problem*

An ASS pipe in a shutdown cooling system of a Korean standard nuclear power plant was considered. The pipe was made of SA312 TP316 stainless steel with an outer radius of 205.61 mm and a wall thickness of 38.34 mm. The pipe includes a weldment made of ER316L. Fig. 1 shows the schematics of a typical shutdown cooling system pipe and the weldment. Physical and mechanical properties (density, specific heat, thermal conductivity, thermal expansion coefficient, elastic modulus, Poisson's ratio, yield strength, and ultimate tensile strength) needed for residual stress FE analyses were taken from ASME Sec. II [14], manufacturer's database [15], and the literature [16]. For TP316 and ER316L, latent heat is 300 kJ/kg and Poisson's ratio 0.27. In order to consider relaxation of stress and plastic strains for the welding simulation, the annealing temperature was set at 1,460°C, which is the melting temperature.

SIF RR analyses were conducted for two types of inner surface cracks, semicircular circumferential surface cracks and fully circumferential surface cracks, in order to evaluate the differences in SIFs according to the applied methods, such as FE analyses and FFS assessment codes as well as evaluators. The normalized crack depths to thickness ratios ($a/t$) are 0.3 and 0.6 for both types of cracks, and the ratio of crack depth to crack length ($a/2c$) is 0.5 for semicircular cracks.

### 2.2. *FE analyses for determination of reference residual stresses*

To determine reference residual stresses, FE analyses were carried out based on well-established procedures for welding simulation [8,13]. In particular, residual stresses were calculated from sequentially coupled heat transfer and thermal stress analyses using the commercial software ABAQUS [17]. Fig. 2A shows the 3-D FE model and welding beads used for simulation, which consisted of eight-node linear brick elements (DC3D8) for heat transfer analyses and eight-node linear brick elements with reduced integration (C3D8R) for thermal stress analyses. The numbers of nodes and elements were 103,806 and 96,264, respectively.

There are two representative methods for attaching weld beads: the prescribed temperature method and the volumetric flux method [8]. The prescribed temperature method is to apply heat to each weld bead by maintaining the set temperature at 10°C higher than the melting point ($T_m$) of a material for a designated time, and this method showed little difference compared with the volumetric flux method [8]. For efficiency in preparing the input deck and computational time, the prescribed temperature method was adopted in the present study. The melting temperature of TP316 and ER316L is 1,460°C and the set temperature is 1,470°C. The sustaining time of the welding process was determined from repeated heat transfer analyses as the optimum result to provide equivalent temperature distributions at a location of 4 mm from the fusion line [8,13]. Then, thermal stress analyses were conducted by employing temperature profiles obtained from the heat transfer analyses; axial stress

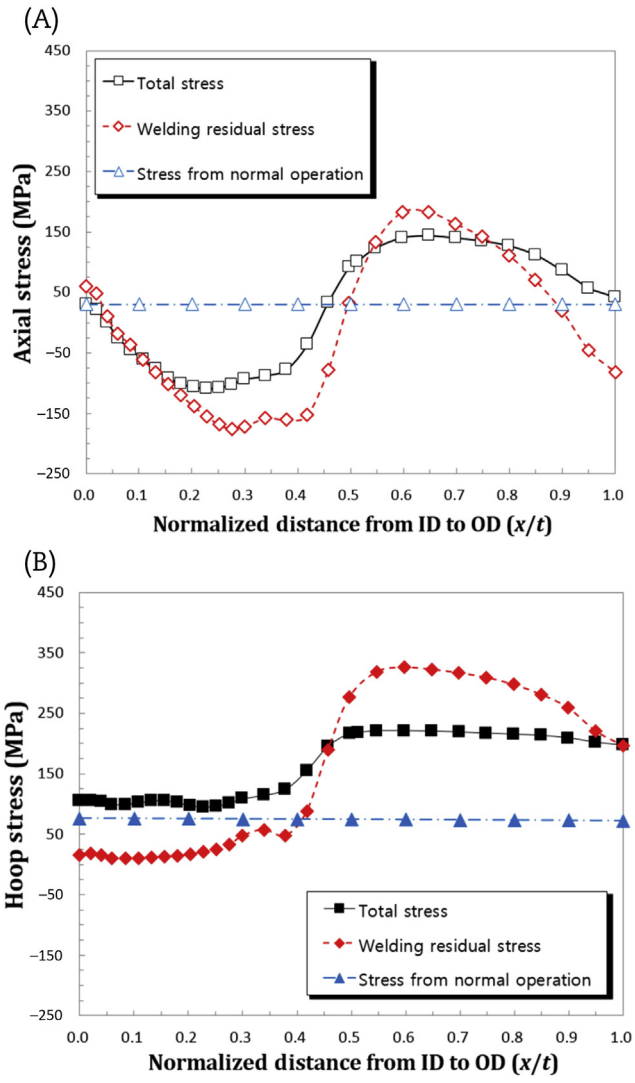


**Fig. 3 – Comparison of stress components. (A) Axial stress. (B) Hoop stress. ID, inner diameter; OD, outer diameter.**

distribution as a representative result after the welding is depicted in Fig. 2B.

### 2.3. FE analyses for determination of reference SIFs

FE analyses to determine reference SIFs were carried out, which considered the welding residual stress and operational stress caused by the normal operating condition of the shutdown cooling system. A temperature of 327.3°C and an internal pressure of 15.5 MPa were applied as normal operating conditions, and total stress distributions along the normalized distance from inner to the outer diameter were obtained as shown in Fig. 3. For the cracked pipes, by considering symmetricity, quarter models were generated. To avoid problems associated with incompressibility, the reduced integration 20-node element (element type C3D20R in ABAQUS element library) was used. Fig. 4 illustrates representative FE models for inner surface crack evaluation; the numbers of nodes ranged from 17,652 to 30,670 for the semicircular circumferential crack and was 100,775 for the fully circumferential crack. The number of elements ranged from 3,849 to 6,732 for the semicircular circumferential crack, and was 23,280 for the fully circumferential crack. Prior to calculating SIFs, total stress distributions were mapped into FE models of the cracked pipes using the "MAP SOLUTION" option, ABAQUS. Fig. 5 shows a comparison of residual stress distributions obtained from simulation and mapping to the cracked FE model. The differences are relatively small.

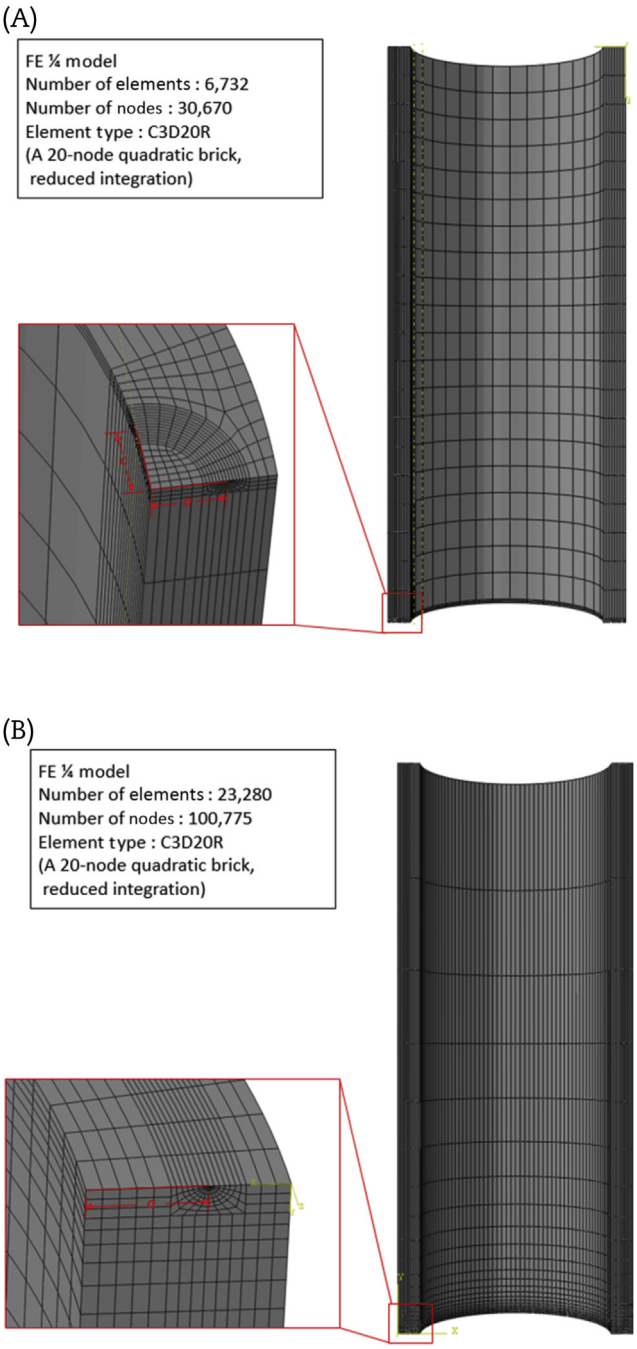


**Fig. 4 – Representative FE models for crack evaluation. (A) Semicircular circumferential; $a/2c = 0.5$, $a/t = 0.6$. (B) Fully circumferential; $a/t = 0.6$. FE, finite element.**

## 3. SIF RR evaluation

### 3.1. SIF solutions in FFS assessment codes

Total stress distributions through wall thickness, obtained from the previous FE analyses, were provided to RR participants, and each of them calculated SIFs of the welded ASS pipes with a semicircular or fully circumferential surface crack according to the procedures in ASME Sec. XI [9], API 579-1 [10], and R6 [11] codes. Approaches employed in RR analyses are summarized in Table 1; the key characteristics of the three codes and embedded equations were reviewed.

ASME Sec. XI suggests two SIF calculation methods. One is a polynomial method and the other is a linearization method. Eq. (1) describes the SIF solution of surface cracked pipe, and Eq. (2) is an equation for the flaw shape parameter Q.

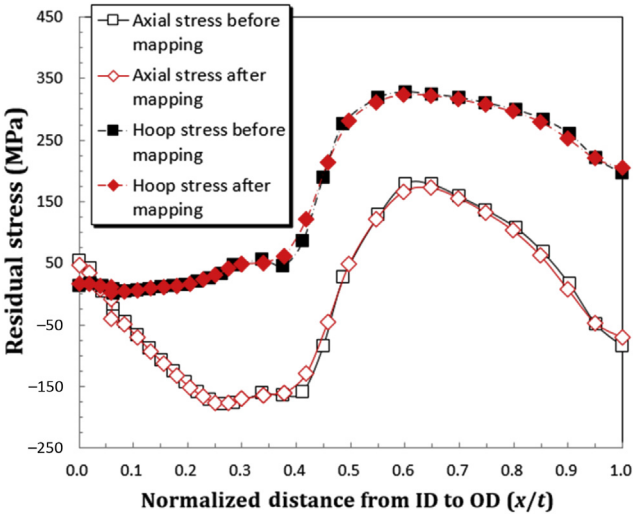


**Fig. 5 – Comparison of residual stresses.**

**Table 1 – Approaches employed in SIF RR analyses.**

| Participant | Evaluation method | |
|---|---|---|
| P1 | FE analyses | ABAQUS |
| | ASME Sec. XI | Linearization method |
| | API 579-1 | Fourth-order polynomial equation |
| P2 | ASME Section XI | Third-order polynomial equation |
| | API 579-1 | Fourth-order polynomial equation |
| | R6 | Third-order polynomial equation |
| P3 | ASME Section XI | Third-order polynomial equation |
| | R6 | Third-order polynomial equation |

API, American Petroleum Institute; ASME, American Society of Mechanical Engineers; FE, finite element; RR, round robin; Sec., section; SIF, stress intensity factor.

$$K_I = [(\sigma_0 + A_P)G_0 + \sigma_1 G_1 + \sigma_2 G_2 + \sigma_3 G_3]\sqrt{\frac{\pi a}{Q}} \quad (1)$$

$$Q = 1 + 4.593\left(\frac{a}{2c}\right)^{1.65} - q_y \quad (2)$$

where $G_i$ ($i = 0, 1, 2, \text{and } 3$) are influence coefficients and $\sigma_i$ ($i = 0,1,2, \text{and } 3$) are stress distribution coefficients. $A_P$ is the applied internal pressure. Eq. (3) describes stresses fitted over the crack depth by the third-order polynomial equation; $q_y$ is the plastic zone correction factor calculated by Eq. (4).

$$\sigma = \sigma_0 + \sigma_1\left(\frac{x}{a}\right) + \sigma_2\left(\frac{x}{a}\right)^2 + \sigma_3\left(\frac{x}{a}\right)^3 \quad (3)$$

$$q_y = \left[\frac{\sigma_0 G_0 + A_P G_0 + \sigma_1 G_1 + \sigma_2 G_2 + \sigma_3 G_3}{\sigma_{ys}}\right]^2 \Big/ 6 \quad (4)$$

The linearization method is used for calculating SIFs using membrane stress and bending stress from the stress distribution through wall thickness, and is described in Eqs. (5) and (6).

$$K_I = [(\sigma_m + A_P)M_m + \sigma_b M_b] \Big/ \sqrt{\frac{\pi a}{Q}} \quad (5)$$

$$q_y = \left[\frac{\sigma_m M_m + A_P M_m + \sigma_b M_b}{\sigma_{ys}}\right]^2 \Big/ 6 \quad (6)$$

where $\sigma_m$ and $\sigma_b$ are membrane and bending stress coefficients, and $M_m$ and $M_b$ are SIF influence coefficients.

API 579-1 also suggests the polynomial method. Stresses are fitted over the entire wall thickness by a fourth-order polynomial equation, as given in Eq. (7). The SIF solution for the semicircular circumferential surface crack is described by Eq. (8), while Eq. (10) represents the SIF solution for the fully circumferential surface crack. Here, the plastic zone correction factor incorporated in ASME Sec. XI was not considered.

$$\sigma(x) = \sigma_0 + \sigma_1\left(\frac{x}{t}\right) + \sigma_2\left(\frac{x}{t}\right)^2 + \sigma_3\left(\frac{x}{t}\right)^3 + \sigma_3\left(\frac{x}{t}\right)^4 \quad (7)$$

$$K_I = \left[(\sigma_0 + A_p)G_0 + \sigma_1 G_1\left(\frac{a}{t}\right) + \sigma_2 G_2\left(\frac{a}{t}\right)^2 + \sigma_3 G_3\left(\frac{a}{t}\right)^3 + \sigma_4 G_4\left(\frac{a}{t}\right)^4\right]\sqrt{\frac{\pi a}{Q}} \quad (8)$$

$$Q = 1 + 1.464\left(\frac{a}{c}\right)^{1.65} \quad (9)$$

$$K_I = \left[(\sigma_0 + A_p)G_0 + \sigma_1 G_1\left(\frac{a}{t}\right) + \sigma_2 G_2\left(\frac{a}{t}\right)^2 + \sigma_3 G_3\left(\frac{a}{t}\right)^3 + \sigma_4 G_4\left(\frac{a}{t}\right)^4\right]\sqrt{\pi a} \quad (10)$$

The third-order polynomial equation suggested by R6 is similar to that of ASME Sec. XI. Eqs. (11) and (12) describe SIF solutions for the semicircular and fully circumferential surface cracks, respectively. However, the internal pressure and plastic zone correction factor are not considered.

$$K_I = \sqrt{\pi a}\left[\sum_{i=0}^{3}\sigma_i f_i\left(\frac{a}{t}, \frac{2c}{a}, \frac{R_i}{t}\right) + \sigma_{bg} f_{bg}\left(\frac{a}{t}, \frac{2c}{a}, \frac{R_i}{t}\right)\right] \quad (11)$$

$$K_I = \frac{1}{\sqrt{2\pi a}}\int_0^a \sigma(x)\sum_{i=1}^{3} f_i\left(\frac{a}{t}, \frac{R_i}{t}\right)\left(1 - \frac{x}{a}\right)^{\left(i-\frac{3}{2}\right)} dx \quad (12)$$

where $f_i$ and $f_{bg}$ are flaw shape parameters, and $\sigma_{bg}$ is the global bending stress.

### 3.2. Comparison of SIFs

SIFs estimated from RR analyses by ASME Sec. XI, API 579-1, and R6 are summarized in Table 2, and SIFs obtained from FE analyses are summarized in Table 3. Fig. 6 depicts the comparisons of SIFs estimated by FFS assessment codes as well as FE analyses. As shown in the figure, estimation results were dependent on participants. These discrepancies were caused by unique features in each code as well as the mistakes of participants, such as not considering the decreased yield strength with increasing temperature and not interpolating SIF influence coefficients. Negative SIFs were calculated for circumferentially cracked pipes with 0.3 of $a/t$, which is mainly caused by the compressive residual stresses near the inner surface of pipes. The effects of the interpolation were not significant.

Conversely, SIFs estimated by ASME Sec. XI showed a different trend from those by other methods. Especially, the linearization method in ASME Sec. XI provided very conservative results compared with the polynomial method, as $a/t$ increased. The maximum difference of SIFs between the two methods for the semicircular circumferential surface crack

**Table 2 – SIFs estimated from initial RR analyses by FFS assessment codes.**

SIF($MPa\sqrt{m}$)

| Participant | Semicircular circumferential surface crack | | | | | |
|---|---|---|---|---|---|---|
| | $a/2c = 0.5$, $a/t = 0.3$ | | | $a/2c = 0.5$, $a/t = 0.6$ | | |
| | ASME Sec. XI | API 579-1 | R6 | ASME Sec. XI | API 579-1 | R6 |
| P1 | −5.33 (linearization) | −7.27 | – | 23.71 (linearization) | 9.23 | – |
| P2 | −7.87 (polynomials) | −5.97 | −9.71 | 5.81 (polynomials) | 7.20 | 3.28 |
| P3 | −10.81 (polynomials) | – | −10.62 | 5.13 (polynomials) | – | 5.54 |
| | Fully circumferential surface crack | | | | | |
| | $a/t = 0.3$ | | | $a/t = 0.6$ | | |
| | ASME Sec. XI | API 579-1 | R6 | ASME Sec. XI | API 579-1 | R6 |
| P1 | −7.46 (linearization) | −12.10 | – | 282.99 (linearization) | −2.39 | – |
| P2 | −16.33 (polynomials) | −10.99 | – | −17.21 (polynomials) | 2.65 | – |
| P3 | −22.22 (polynomials) | – | −17.68 | −32.47 (polynomials) | – | −1.69 |

API, American Petroleum Institute; ASME, American Society of Mechanical Engineers; FFS, fitness for service; RR, round robin; Sec., section; SIF, stress intensity factor.

with $a/t = 0.6$ was 308%, as marked in Fig. 6A. A similar trend was observed for the fully circumferential surface crack, as shown in Fig. 6B, in which high-valued data could not be represented.

Fig. 7 shows the revised RR results after correcting the aforementioned mistakes, and the SIFs calculated by each RR participant agreed well. For instance, the maximum difference of SIFs between the two methods in ASME Sec. XI was reduced by 146% for the semicircular circumferential surface crack with $a/t = 0.6$, and the discrepancy depicted as a red arrow mark in Fig. 6B also decreased. Among the FFS codes, R6 was selected as a plausible optimized procedure for SIF evaluation because its results were quite close to the reference FE analysis data. However, for practical application of these codes, further examinations are required in relation to different orders and ranges for fitting the stress distributions, consideration of internal pressure, and combination of SIFs.

## 4. Sensitivity analyses

As discussed in the previous section, estimated SIFs differ depending on the applied FFS codes and participants. Since the participants reached a consensus on appropriate procedures of FE analysis and FFS code application, subsequent sensitivity analyses as well as supplementary evaluation for $a/t = 0.4$, 0.5, and 0.8 were carried out by the organizer (participant P1) to confirm the SIF trends and examine the effects of variables. The major variables that can affect the SIF calculation were evaluated by the two FFS assessment codes, and their results are summarized in Table 4 and depicted in Figs. 8–10.

**Table 3 – SIFs obtained from FE analyses.**

| Type of crack | | SIF($MPa\sqrt{m}$) |
|---|---|---|
| Semicircular circumferential surface crack | $a/2c = 0.5$, $a/t = 0.3$ | −11.46 |
| | $a/2c = 0.5$, $a/t = 0.6$ | 4.39 |
| Fully circumferential surface crack | $a/t = 0.3$ | −17.52 |
| | $a/t = 0.6$ | 0.25 |

FE, finite element; SIF, stress intensity factor.

### 4.1. *Fitting of stress distribution*

In order to fit the stress distributions, R6 employed the third-order polynomial equation over the range until the crack depth, while API 579-1 employed the fourth-order polynomial equation over the entire wall thickness. Even though the latter method has the advantage that it requires only one trial for stress fitting regardless of crack sizes, it may lead to an inadequate fit over the whole section. Fig. 8 compares the total stress distributions obtained from 3-D FE analyses and two polynomials, and stress distributions of $a/t = 0.4$, 0.5, and 0.8 were added to help decide which polynomial is better. Only axial stresses were examined because they are the governing components for the circumferential cracks dealt with in this study.

Overall, even though the differences were not significant, fitting the stresses using the third-order polynomial equation until the crack depth gave better similitude to the reference FE analysis results. In particular, the differences of total stresses obtained from the two polynomials increased near the inner surface and crack tip, and the maximum difference was 68%. Therefore, the third-order polynomial equation until the evaluating crack depth is recommended for estimating the stress distribution of welded ASS pipes. Another reason for this recommendation can be found in the consistent use of FFS codes for subsequent SIF estimation, which will be discussed in the following section.

### 4.2. *Consideration of internal pressure*

As SIF solutions, API 579-1 considers internal pressure ($A_p$) in Eqs. (8) and (9), whereas R6 does not take it into account in Eqs. (11) and (12). Fig. 9 compares SIFs according to whether the

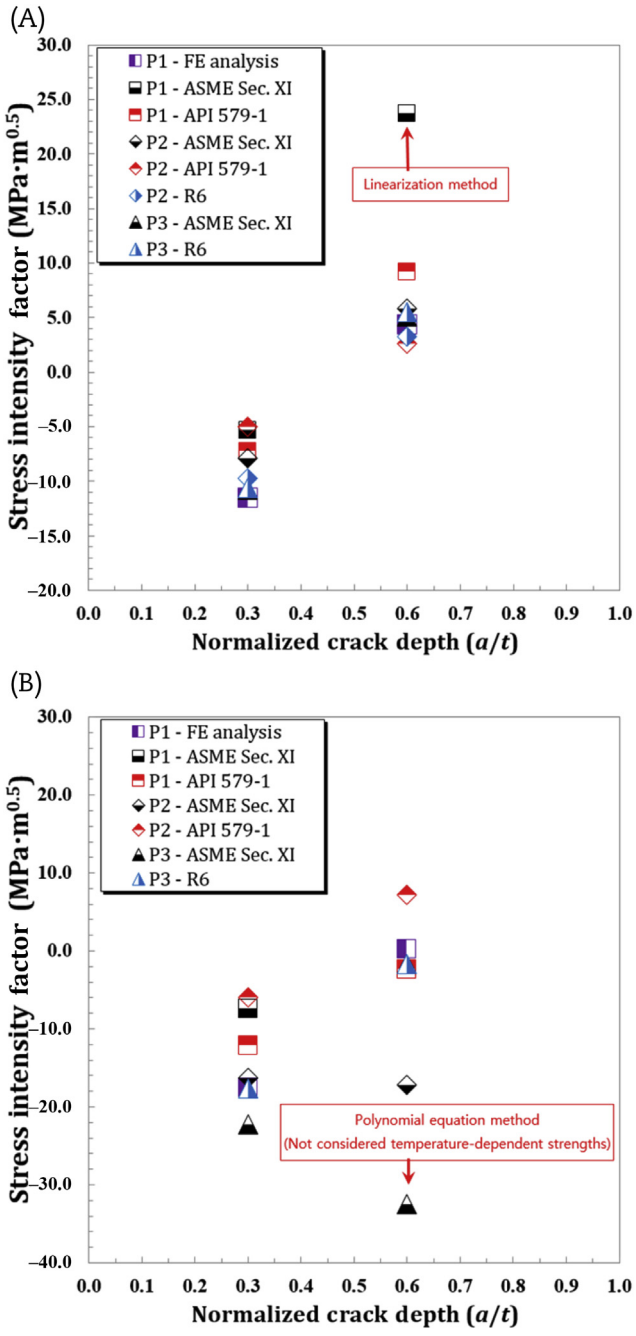


**Fig. 6 – SIFs of welded ASS pipes with a circumferential inner surface crack. (A) Semicircular circumferential surface crack. (B) Fully circumferential surface crack. ASME, American Society of Mechanical Engineers; FE, finite element; SIF, stress intensity factor.**

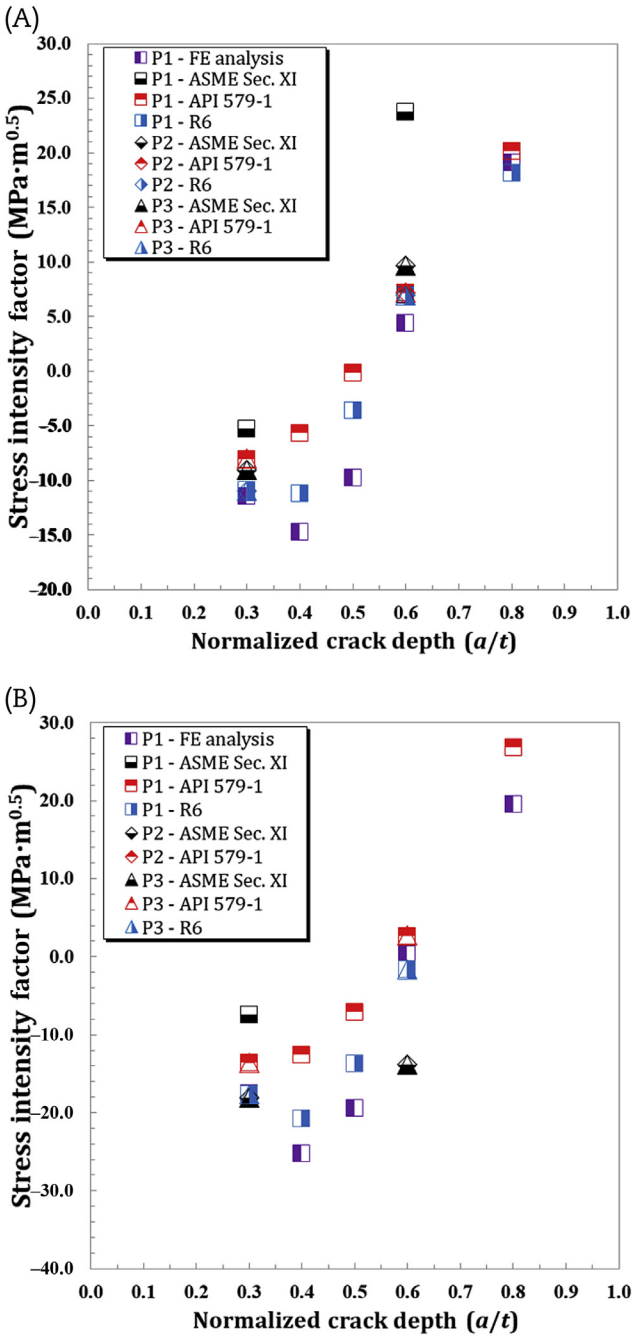


**Fig. 7 – Revised SIFs after resolving mistakes found in initial RR analyses. (A) Semicircular circumferential surface crack. (B) Fully circumferential surface crack. ASME, American Society of Mechanical Engineers; FE, finite element; RR, round robin; SIF, stress intensity factor.**

internal pressure is applied or not for the two types of inner surface circumferential cracks. SIF values increased with the normalized crack depths. This trend was remarkable when absolute SIF values were high and the flaw shape was fully circumferential.

If we focus more on the more realistic semicircular circumferential surface crack than on the fully circumferential surface crack, due to the internal pressure, SIF values increased by 20% in the case of API 579-1 and 18% in the case of R6 when $a/t = 0.3$, and 70% in the case of API 579-1 and 42% in the case of R6 when $a/t = 0.6$. This means that the use of R6 with the internal pressure led to conservative SIFs, while adequate use of the internal pressure provided SIFs comparable with the FE analysis data. Therefore, internal pressure should be treated carefully for an accurate estimation of SIFs according to specific FFS codes.

**Table 4 – Sensitivity analysis results of SIF estimations.**

| SIF(MPa$\sqrt{m}$) | | | | |
|---|---|---|---|---|
| Case | Semicircular circumferential surface crack | | | |
| | $a/2c = 0.5$, $a/t = 0.3$ | | $a/2c = 0.5$, $a/t = 0.6$ | |
| | API 579-1 | R6 | API 579-1 | R6 |
| 1 (w/$A_P$) | −8.08 | −8.94 | 7.20 | 9.79 |
| 2 (w/o $A_P$) | −10.05 | −10.93 | 4.24 | 6.87 |
| | Fully circumferential surface crack | | | |
| | $a/t = 0.3$ | | $a/t = 0.6$ | |
| 1 (w/$A_P$) | −13.67 | −13.94 | 2.64 | 5.14 |
| 2 (w/o $A_P$) | −17.52 | −17.67 | −4.53 | −1.69 |

API, American Petroleum Institute; SIF, stress intensity factor; w/, with; w/o, without.

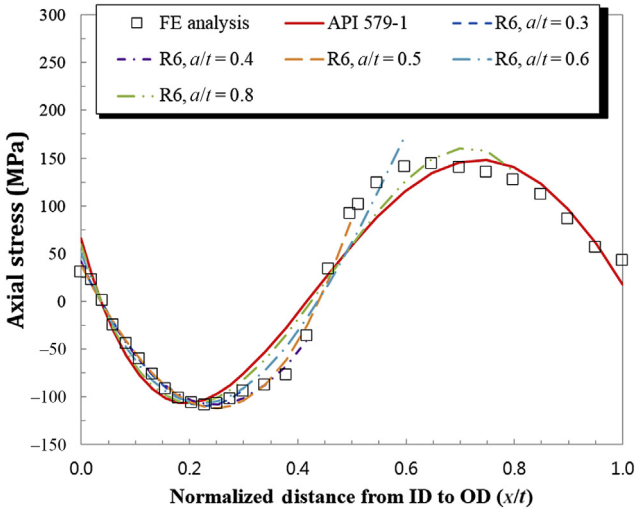


**Fig. 8 – Comparison of total stress distributions obtained from FE analyses and polynomials. FE, finite element; ID, inner diameter; OD, outer diameter.**

### 4.3. *Combination of SIFs*

SIFs can be estimated either from the total stress distribution directly (direct calculation) or by a combination of the stress distributions (combined calculation). Fig. 10 compares SIFs determined by the two calculations, the results of which can be classified into three regions. Direct calculations provided lower SIFs until $a/t = 0.3$, comparable or higher SIFs when $0.3 < a/t < 0.6$, and lower SIFs after $a/t = 0.6$ compared with the combined calculations. These complex trends seemed to be closely related to the residual stress profiles produced by welding, which showed compressive stress fields until approximately $a/t = 0.5$. In addition, the trend can be regarded as general for ASS welds of nuclear piping despite the fact that the details may be slightly different because the geometry and operating conditions adopted in this study are similar to those of other high-energy line piping.

If we focus also on the semicircular surface crack, based on FE analysis data, the difference of SIF values were 7% in the case of API 579-1 and 37% in the case of R6 until $a/t = 0.3$, 58% in the case of API 579-1 and 35% in the case of R6 when $0.3 < a/t < 0.6$, and 12% in the case of API 579-1 and 18% in the case of R6 after $a/t = 0.6$. The differences are not ignorable, especially for a medium-size crack of $a/t = 0.4$. To resolve this issue, Eqs. (11) and (12) in the R6 code were modified by taking into account the applied internal pressure ($A_P$) and represented by expanding forms as follows:

$$K_I = \sqrt{\pi a}\left[(\sigma_0 + A_P)f_0 + \sigma_1 f_1 + \sigma_2 f_2 + \sigma_3 f_3 + \sigma_{bg} f_{bg}\right] \tag{13}$$

$$K_I = \frac{1}{\sqrt{2\pi a}}\left[\left(2g_0 + \frac{2}{3}g_1 + \frac{2}{5}g_2 + \frac{2}{7}g_3\right)f_1 + \left(\frac{2}{3}g_0 + \frac{2}{5}g_1 + \frac{2}{7}g_2 + \frac{2}{9}g_3\right)f_2 + \left(\frac{2}{5}g_0 + \frac{2}{7}g_1 + \frac{2}{9}g_2 + \frac{2}{11}g_3\right)f_3\right] \tag{14}$$

where $g_0 = ((\sigma_0 + A_P) + \sigma_1 + \sigma_2 + \sigma_3)$, $g_1 = (-\sigma_1 - 2\sigma_2 - 3\sigma_3)$, $g_2 = (\sigma_2 + 3\sigma_3)$, and $g_4 = -\sigma_3$ are integration constants.

The resultant SIFs of semicircular surface cracks in Fig. 10A shows similar and conservative trends compared with the reference FE analysis data. Moreover, Fig. 10B represents consistent trends for the fully circumferential surface cracks, in which evaluation data of $a/t = 0.8$ by R6 were not indicated because relevant SIF influence coefficients of this type of crack are provided until $a/t = 0.6$. Meanwhile, engineering design and structural integrity evaluation practices generally consider decomposed primary, secondary, and residual stresses. Therefore, the use of the combined calculation by the modified R6 can be recommended, taking into account the applied internal pressure based on the similarity and conservatism compared with detailed FE analysis results.

## 5. Conclusions

In this study, RR analyses on SIFs were carried out to examine the appropriateness of structural integrity assessment methods for ASS pipes with two types of inner surface circumferential cracks. Resulting estimations were compared with those obtained by 3-D FE analyses, and the effects of major variables were quantified, from which the following conclusions were made:

(1) RR analysis results showed that the linearization method and the polynomial method in ASME Sec. XI tend to estimate very conservative results as the normalized crack depth increases. For example, the maximum difference of SIFs between the two methods for the semicircular circumferential surface crack with $a/t = 0.6$ was 150% approximately.
(2) Fitting the stresses using a third-order polynomial equation until the crack depth gave better similitude to the reference FE analyses data than the fourth-order polynomial equation over the entire wall thickness. In particular, the differences of total stresses obtained from the two polynomials increased near the inner surface and crack tip.
(3) Among the FFS codes, the modified R6 considering the applied internal pressure was selected as the optimized

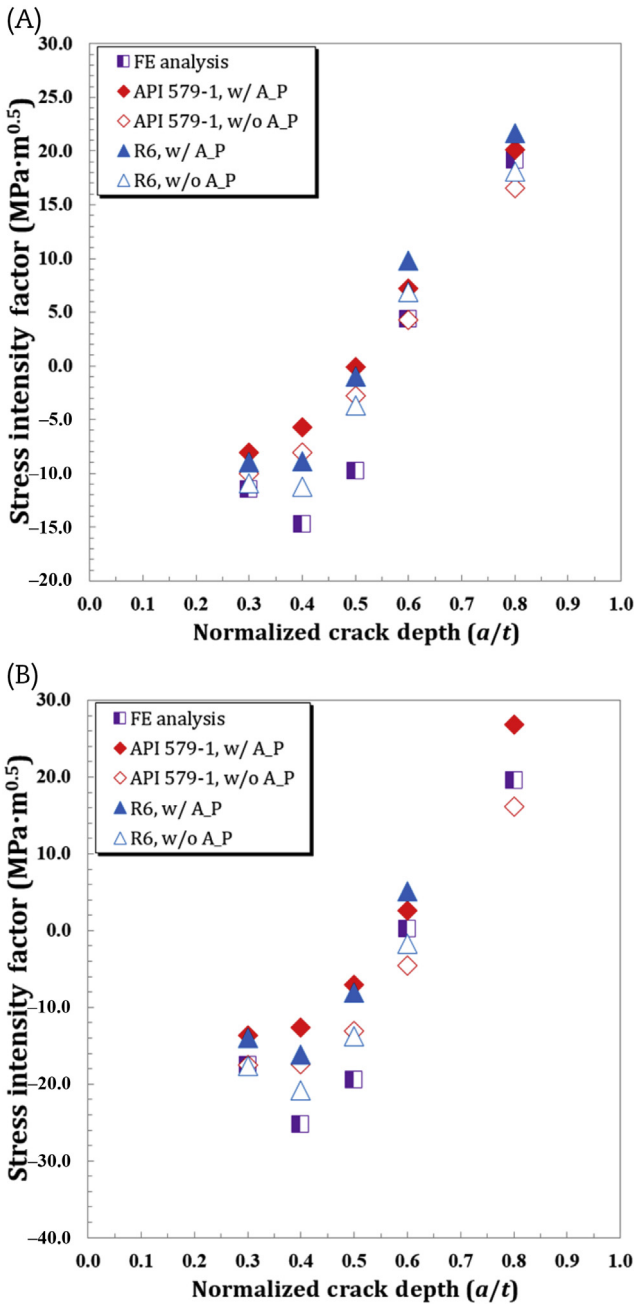


**Fig. 9 – Comparison of SIFs according to internal pressure. (A) Semicircular circumferential surface crack. (B) Fully circumferential surface crack. FE, finite element; SIF, stress intensity factor.**

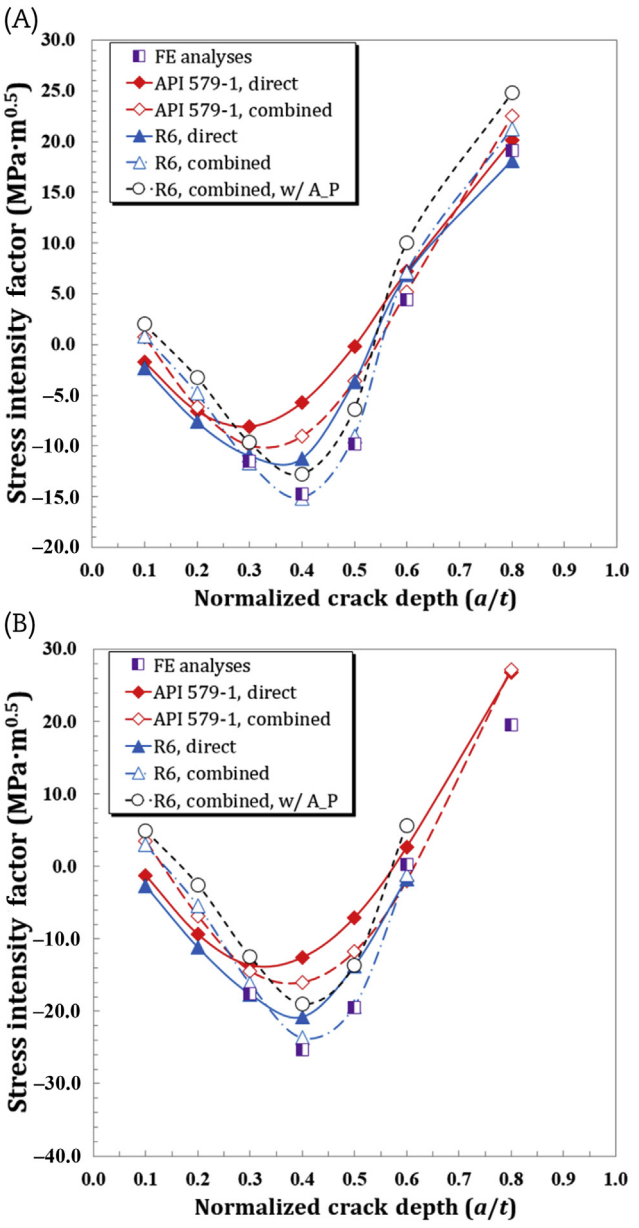


**Fig. 10 – Comparison of SIFs between direct and combined calculations. (A) Semicircular circumferential surface crack. (B) Fully circumferential surface crack. FE, finite element; SIF, stress intensity factor.**

procedure for the SIF evaluation because its results were similar to and conservative compared with the reference FE analysis data.

(4) SIFs can be estimated either from the total stress distribution directly or by a combination of stress distributions. In this study, the latter is recommended because engineering design and structural integrity evaluation practices generally take into account decomposed primary, secondary, and residual stresses.

## Conflicts of interest

All contributing authors declare no conflicts of interest.

## Acknowledgments

This research was supported by the project "Development of the Evaluation and Mitigation Technology against Degradation of the Nuclear Pressure Vessel and Piping (I)" through Korea Hydro & Nuclear Power Company and by the energy R&D program through the Korea Institute of Energy Technology Evaluation and Planning (KETEP, Seoul, Korea), and was granted financial resources by the Ministry of Trade, Industry

and Energy (MOTIE; Sejong, Republic of Korea; Grant No. 20141510101640).

## Nomenclature

| | |
|---|---|
| $A_P$ | Internal pressure (MPa) |
| $a$ | Crack depth (mm) |
| $c$ | Half of crack length (mm) |
| $E$ | Elastic modulus (GPa) |
| $g_i$ | Integration coefficients |
| $G_i$ | SIF influence coefficients |
| $K_I$ | SIF(MPa$\sqrt{m}$) |
| $M_b$ | SIF coefficient for bending stress |
| $M_m$ | SIF coefficient for membrane stress |
| Q | Flaw shape parameter |
| $q_y$ | Plastic zone correction factor |
| $R_i$ | Inner radius of pipe (mm) |
| $t$ | Wall thickness (mm) |
| $T_m$ | Material melting temperature (°C) |

*Greek symbols*

| | |
|---|---|
| $\sigma_b$ | Bending stress (MPa) |
| $\sigma_{bg}$ | Global bending stress (MPa) |
| $\sigma_i$ | Stress distribution coefficients |
| $\sigma_m$ | Membrane stress (MPa) |
| $\sigma_{ys}$ | Specified minimum yield strength (MPa) |

## REFERENCES


[1] R.C. Wimpory, F.R. Biglari, R. Schneider, K.M. Nikbin, N.P. O'Dowd, Effect of residual stress on high temperature deformation in a weld stainless steel, Mater. Sci. Forum 524–525 (2006) 311–316.

[2] H. Moshayedi, I. Sattari-Far, The effect of welding residual stresses on brittle fracture in an internal surface cracked pipe, Int. J. Press. Vessels Piping 126–127 (2015) 29–36.

[3] K. Chandra, V. Kain, V. Bhutani, V.S. Raja, R. Tewari, G.K. Dey, J.K. Chakravartty, Low temperature thermal aging of austenitic stainless steel welds: kinetics and effects on mechanical properties, Mater. Sci. Eng. A 534 (2012) 163–175.

[4] P.K. Singh, V. Bhasim, R.K. Singh, R. Singh, G. Das, Low temperature thermal ageing embrittlement in austenitic stainless steel weld, Trans. Struct. Mech. Reactor Technol. 23 (2015) 305.

[5] K.S. Lee, W. Kim, J.G. Lee, Assessment of possibility of primary water stress corrosion cracking occurrence based on residual stress analysis in pressurizer safety nozzle of nuclear power plant, Nucl. Eng. Technol. 44 (2012) 343–354.

[6] J.D. Hong, C.H. Jang, T.S. Kim, PFM application for the PWSCC integrity of Ni-base alloy welds—development and application of PINEP-PWSCC, Nucl. Eng. Technol. 44 (2012) 961–970.

[7] T. Ogawa, M. Itatani, T. Saito, T. Hayashi, C. Narazaki, K. Tsuchihashi, Fracture assessment for a dissimilar metal weld of low alloy steel and Ni-base alloy, Int. J. Press. Vessels Piping 90–91 (2012) 61–68.

[8] S.H. Lee, Y.S. Chang, S.W. Kim, Residual stress assessment of nickel-based alloy 690 welding parts, Eng. Fail. Anal. 54 (2015) 57–73.

[9] ASME, ASME Boiler and Pressure Vessel Code, Section XI, Rules for Inservice Inspection of Nuclear Power Plant Components, App. A, 2010.

[10] American Petroleum Institute, API 579–1/ASME FFS-1, Fitness-for-Service, 2007.

[11] British Energy, R6-Assessment of the Integrity of Structures Containing Defects, Revision 4, 2010.

[12] S. Marie, C. Faidy, K.J. Bench, Benchmark on Analytical Calculation of Fracture Mechanics Parameters KI and J for Cracked Piping Components—Progress of the Work, Proceedings of the ASME Pressure Vessels & Piping Conference PVP2013, 2013, p. 97178.

[13] KHNP, Standard Procedure for Finite Element Residual Stress Analysis, 2010.

[14] ASME, ASME Boiler and Pressure Vessel Code, Section II, Part D, Properties, 2004.

[15] AK Steel Corporation, 316/316L Stainless Steel Product Data Bulletin [Internet]. 2013 [cited 2014 Oct 28]. Available from: http://www.aksteel.com/pdf/markets_products/stainless/austenitic/316_316l_data_bulletin.pdf (accessed 28.10.14).

[16] M. Smith, A. Smith, NET Task Group 1 Single Weld Bead on Plate: Review of Phase 1 Weld Simulation Round Robin. Appendix A—Protocol for Finite Element Simulations of the NET Single-Bead-on-Plate Test Specimen, Report E/REP/BDBB/0089/GEN/05, British Energy Generation Ltd, 2006.

[17] Dassault Systems, ABAQUS, Version 6–13.1, 2013.